Journal of Applied Polymer Science

Statistical Analysis of Nanofibers Alignment in Magnetic-Field-Assisted Electrospinning Including an Alignment Percentage Formula

Shahrzad Rahmani, Mehdi Rafizadeh, Framarz Afshar Taromi
Nano and Smart Polymers Center of Excellence, Department of Polymer Engineering and Color Technology, Amirkabir University of Technology, Tehran, Iran
Correspondence to: M. Rafizadeh (E-mail: Mehdi@aut.ac.ir)

ABSTRACT: Magnetic-field-assisted electrospinning (MFAES) is a simple and effective method to align polymer nanofibers. In this method, further research is needed to identify alignment mechanism. Hence, this article includes statistical analysis of affecting factors to investigate alignment mechanism in MFAES. Tip to target distance, magnets distance, voltage, and collection time, which are recognized as the most effective factors on nanofibers alignment, were applied in design of experiments. Central composite method was applied to get required experiments with designed expert 8 software. A response surface was proposed with regression coefficient of 97%. Then, the common physics concepts and statistical results were used to discuss the affecting mechanism of the electric and magnetic fields on the electrospinnig jet and the nanofibers alignment. Field emission scanning electron microscopy images were used to characterize the nanofibers alignment and calculate overall alignment percentage using a proposed statistical combinatorial weighted percentage formula. MFAES method, used in this research, achieved 95.3% polyacrylonitrile-aligned nanofibers. © 2014 Wiley Periodicals, Inc. J. Appl. Polym. Sci. **2014**, *131*, 41179.

KEYWORDS: electrospinning; fibers; nanostructured polymers

Received 6 March 2014; accepted 16 June 2014
DOI: 10.1002/app.41179

INTRODUCTION

Fibers with diameters <300 nm are called nanofibers. In the recent decade, various fields have been suggested as potential applications for nanofibers.[1,2] Tissue engineering,[3] filtration,[4] bio sensors,[5] protective clothing,[6] energy generation applications,[7] membrane and cosmetics[8] are some of these applications. Therefore, many studies have been concentrated on nanofibers subjects. Moreover, mass production of nanofibers is expected to be expanded in the near future.

Electrospinning is the most common method to produce continuous nanofibers due to its ease of use and inexpensive set up for producing submicron fibers.[9] Foundation of this process is based on extreme drawing of a polymer solution or melt in a high voltage electric field.[9] Movement of the solution jet, in electric field, has been studied by taking images using high speed camera.[10] It was observed that there is a short straight path in the beginning. Then, the jet goes under an expanding and bending path.[10] Movement in this part of path has some complex pattern that is named whipping or bending instability.[11] Bending instability is due to repulsive force among similar charges on the jet.[10] In addition, there is an induced magnetic field around the bending jet.[12] This magnetic field produces a conical helix path. This conical helix path has the lowest energy level.[13] Solvent evaporates and polymer goes under severe drawing that is thousand times much more than the drawing in the straight path.[9,14] The result is production of non-woven and irregular mat of ultra-fine fibers.[15] Highly aligned PAN nanofibers, as a precursor for carbon fibers, is known crucial for preparing high performance carbon fibers.[16,17] Moreover, aligned nanofibers are necessary for other applications such as composites, electrochemical sensing, tissue engineering, microelectronics, photonics, and so on. So far, several methods have been proposed to align nanofibers and more researches are going on producing much more aligned nanofibers.[15] These methods could be classified as rotating collectors,[15–22] collecting fibers in a gap,[23–26] applying an external magnetic field,[26–30] rotary jet spinning,[31] electrodynamic control of the nanofibers alignment.[32] Among all, the collecting in a gap method has been recognized as a simple and successful method to align nanofibers. In this method, nanofibers are stretched across the gap between two grounded blades (electrode) instead of usual flat collectors. Therefore, the electric field distribution is in favor of nanofibers alignment.[23] It is well known that the collected nanofibers contain positive charges (residual charges) that repel the jet and prevent alignment along the gap.[24] Liu et al.[24] investigated the gap size and showed that the gap size increases alignment. Their simulation results calculated a decrease of 10–25% in alignment due to residual charges on the fibers.

Yang et al.[28] generated aligned nanofibers by electrospinning magnetic nano particle-doped polymer solution in the presence of an

external magnetic field. The external magnetic field was applied using two permanent parallel magnets placed on a grounded target. Therefore, alignment of the nano particles, in the jet inside the magnetic field, causes alignment of the collected nanofibers.[28]

Without adding any magnetic-nano particles, they concluded that electrospun jet behaves as an electrifying solenoid while it moves with whipping toward the target.[28] Whipping of the jet generates a magnetic field. They ascribed nanofibers alignment to interaction between induced magnetic field of the jet motion and external magnetic field. Moreover, the electric field lines deform under influence of magnets.[28]

Liu et al.[33] also used magnetic-field-assisted electrospinning (MFAES) for electrospinning of aligned straight and wavy nanofibers. They showed that by introducing a proper external magnetic field on the collector, large area well-ordered nanofibers could be fabricated with a thick mat. Furthermore, they concluded that MFAES method could produce more uniform nanofibers in comparison to electrospinning without a magnetic field.

Therefore, Although MFAES has been introduced as an effective method for nanofibers alignment, but mechanism of alignment still is a complex phenomenon that requires more studies.[29]

Among the parameters which affect nanofibers alignment, some are well known like: residual charges on collected fibers and electric field distribution.[24] Tip to target distance (distance), voltage, processing time and the size of gap between two magnets (gap size) are the parameters which probably effects on nanofibers alignment in this method.

Response surface method is a statistical based technique that could identify the most effective factors and possible interactions among factors, proposing a surface and optimum condition.[34–36] To study the aforementioned factors, a design of experiments method was used.

To qualify alignment of nanofibers, researchers have suggested different approaches. These approaches include: calculating the nanofibers frequency in two perpendicular directions and taking away angular differences $<90°$,[37] Columns curves with specific interval spaces (e.g., 10°),[38–40] using an Angular Power Spectrum (APS) which is a subset of Fourier power spectrum method (FPSM),[41] and Fast Fourier Transfer (FFT) which has been a noteworthy method in calculating alignment.[42,43] For statistical analysis, it is needed to convert each SEM image to an overall number which alignment could be explained properly. Thus, a new formulation with a numerical output should be determined. This formula should account all the fibers directions and match a coefficient to evaluate overall alignment.

In this research, PAN in dimethyl formamide (DMF) was electrospun. PAN nanofibers were collected in the gap between two grounded magnets. Since studying MFAES mechanism could lead to control and optimize the process, it is proposed to study the effect of four factors: distance, voltage, spinning time and gap on nanofibers alignment. Response surface Method (RSM) based on central composite design (CCD) was used for statistical analysis of parameters effects on alignment percent. A cumulative formulation proposed and used for alignment percentage calculations and 95.3% nanofibers alignment is achieved.

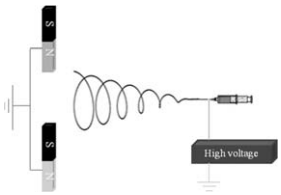

Figure 1. Schematic of electrospinning set up.

EXPERIMENTAL

Materials and Solution Preparation

A PAN copolymer (94% acrylonitrile and 6% methylacrylate with an average molecular weight of 80,000 g/mol) was supplied by Polyacryl Isfahan, Isfahan, Iran. *N,N*-dimethyl formamide (DMF), as solvent, was bought from Merck, Darmstadt, Germany. The copolymer was dissolved in DMF over 2 h at room temperature. No magnetic particles added to the solution. Based on previous results, all the samples had a solution concentration of 12 wt %.[44]

Electrospinning Set-Up

Schematic of the set-up is shown in Figure 1. A high voltage power supply (Gamma High Voltage RR-60 model) was used to supply the required voltage. A syringe pump (New Era Pump System, NE1000) were used to feed the solution at a constant volumetric flow rate of 250 μL/h. Two parallel bars of ferrite magnet ($1 \times 2 \times 5$ cm^3) placed with a gap. Each bar has a surface magnetic field of strength 0.4 T. Spun nanofibers were collected over the gap of two grounded magnets. Then, nanofibers were transferred on an aluminum foil surface for further studies.

Design of Experiments

Twenty-seven experiments were selected using CCD. All calculations were performed using design expert8 software. This designed experiments included 16 cubic points, 8 star points, and 3 center points. Tables I and II gives levels of the selected factors and list of experiments.

Alignment Characterization

Field-emission scanning electron microscopy (Hitachi S4160) was used to characterize the microstructure of the nanofibers. To prepare nanofibers for SEM, they were transferred to an aluminum foil and coated with gold. The acceleration voltage of electron beam was set at 15 kV.

To report that how good the alignment of each SEM image is, it is needed to define a number. So a formula is defined to calculate the alignment percentage of each SEM photo: θ^* is determined as a standard angle which minimizes the sum of squares of all fibre's angle deviations. This standard angle shows the most frequently alignment direction.

$f|\theta_i - \theta^*|$ is the frequency of deviation of nanofibers from standard angle, which i changes from 1 to n (number of nanofibers in the image). $A_j = \{j | j \in 1, 2, \ldots, 90\}$ is a set of measurements for being aligned. The members are the angles among 1°–90°. For example, 90 shows a completely unaligned sample and 0 is related to a completely aligned sample. T_j is determined for calculating the frequency of nanofibers which their deviation from θ^* is less than A_j.

Table I. Factors, Their Levels

Factor	Level 1	Level 2	Level 3	Unit	Code
Voltage	17	19	21	kV	A
Tip-target distance	12	15	18	cm	B
The gap between magnets	1	2	3	cm	C
Collection time	2	3	4	min	D

$$T_j = f|\theta_i - \theta^*| < A_j \quad i = 1, \ldots, n \quad j = 1, \ldots, 90 \tag{1}$$

Then to apply the efficiency of each member of A_j, a weight function (ω_j) is determined. In determining this function, it is noticed that smaller angles in A_j set are more effective on calculating alignment percentage than larger angles.

$$\omega_j = 90 - A_j \Big/ \sum_{j=1}^{90} (90 - A_j) \tag{2}$$

Finally, the overall alignment percentage of each image calculated with the following equation:

$$p = 100 \times \sum_{\substack{i=1,\ldots,n \\ j=1,\ldots,90}} \omega_j T_j / n, \tag{3}$$

These calculations were coded in computing software and overall alignment percentage of the SEM images was calculated.

RESULTS AND DISCUSSION

Figure 2 shows SEM images of aligned electrospun nanofibers. On the contrary, Figure 3 which illustrates a nonwoven mat of the same Nanofibers, make it possible to realize the alignment effectiveness. It is evident that this method can remarkably align nanofibers with no bead. Maximum alignment achieved in this work was 95.3% [Figure 2 (b)]. Figure 2(a,c,d) are selected among all the SEM images of this research, due to high alignment that are 73%, 91%, and 70.5%, respectively. Therefore, this method is not only a simple one, but also effective method.

Based on the DOE analysis, the following quadratic polynomial-model is fitted on data:

$$\begin{aligned} \textit{alignment}\ \% = {} & 80.78 + 1.68A + 6.07B + 2.71C - 6.71D \\ & + 7.66A^2 - 27.87B^2 + 0.35C^2 + 11.97D^2 - 1.16AB \\ & + 6.03AC - 0.40AD - 0.52BC - .84BD + 1.52CD \end{aligned} \tag{4}$$

The R^2, regression coefficient, for this model is equal to 0.9721 that means the model is a very good representation of data. Figure 4 presents the actual alignment values versus predicted alignment values that show consistency among the model and experimental data. The signal to noise, S/N, ratio was 10.969. Values more than 4 indicate an adequate signal and prove that the signal is meaningful in the navigated design space.

P value is a measure of significance of parameters. A comparison of *P* values indicates that B (distance), D (collection time), and AC (the interaction between voltage and gap size) are significant terms in the model (Table III).

One factor effects, the pairwise interactions are shown in Figures 5 and 6, respectively.

Figure 5 Illustrations of one factor effects, horizontal axes are coded values.

Collection Time

It is difficult to experimentally study the effects of residual electrical charges on nanofibers alignment.[24] In this study, passing time has been investigated instead of remained charges effects. Electric conductivity of polymer nanofibers is weak. Therefore, as time passes, with increasing accumulated nanofibers, remained charges accumulate in the gap. These charges deflect the upcoming jet from the electric and magnetic field lines. Thus, the depositing direction changes and alignment decreases.

Figure 5(d) shows the decrease of 10–15% nanofibers alignment with passing time. This is coincidence with Liu et al. simulation results.[24] The statistical analysis resulted a *P* value of 0.0133 which is smaller than 0.05 (Table III) means this factor play relatively an important role in alignment.

Table II. Designed Experiments

	Coded factors			
Experiment number	A	B	C	D
01	21	12	1	2
02	19	18	2	3
03	21	18	3	2
04	21	18	1	4
05	17	12	3	2
06	19	15	2	4
07	17	12	3	4
08	21	12	3	4
09	17	15	2	3
10	21	12	3	2
11	19	15	2	3
12	21	18	1	2
13	19	12	2	3
14	19	15	3	3
15	21	15	2	3
16	19	15	2	2
17	17	12	1	2
18	21	18	3	4
19	17	18	1	4
20	17	18	3	2
21	17	12	1	4
22	19	15	2	3
23	19	15	2	3
24	17	18	1	2
25	21	12	1	4
26	17	18	3	4
27	19	15	1	3

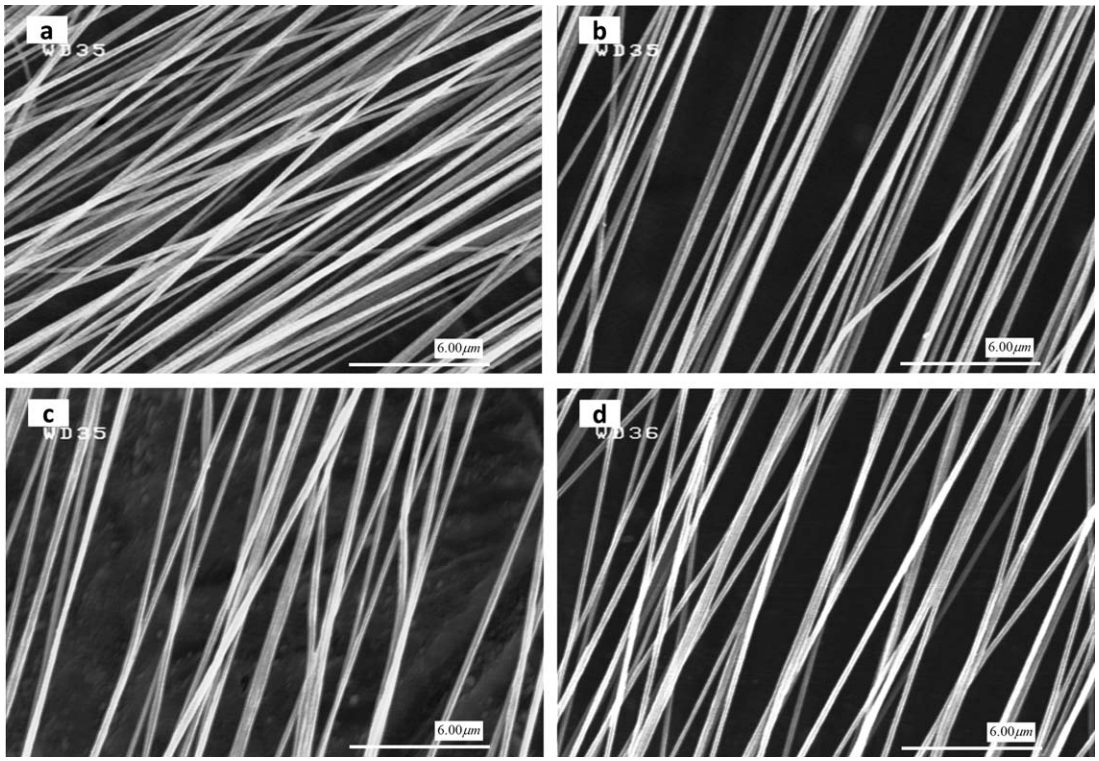

Figure 2. Samples of electrospun aligned nanofibers SEM photographs. (a) 73%, (b) 95.3%, (c) 91%, (d) 70.5%.

It is expectable that voltage and the gap size have interaction with collection time. Voltage affects the jet output flow rate. The gap size determines collecting area. Hence, they could change accumulated charges and nanofibers alignment. But, as it can be seen in Figure 6(c,e,f) there is no mutual interaction between collection time and other factors in the selected working window.

Distance

Figure 5(b) shows two behavior of alignment dependency on distance. At first, alignment increases with distance. Then, alignment begins to decrease.

There are two possible reasons for alignment decrease: Bending instability growth and decrease of directional electric field.

Bending Instability Growth. Bending instability increases with distance. Moreover, the jet begins to move in a spiral like path in smaller scales which results in wavy shaped nanofibers on the target. Figure 7 shows wavy shape nanofibers. This shape is observed in large distances which are due to bending instability development and its regeneration in small segments of the jet. These wavy shaped nanofibers is observed and discussed in published results.[13]

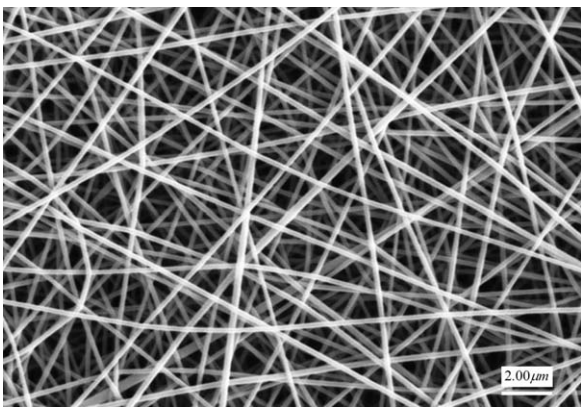

Figure 3. Nanofibers nonwoven mat electrospun from 12 wt % PAN solution at 20 kV and 15 cm tip to target distance.

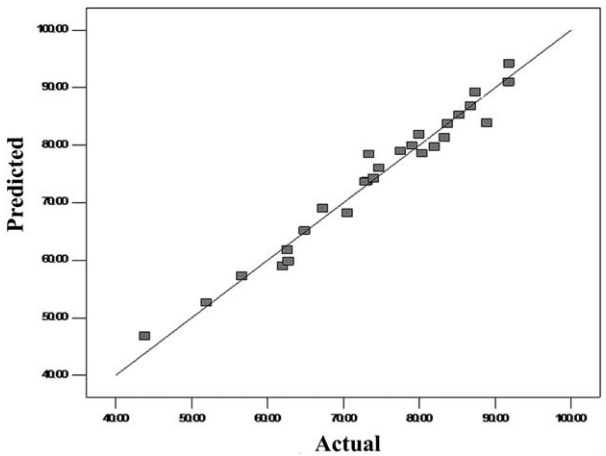

Figure 4. Actual versus predicted values.

Table III. Analysis of Variance (ANOVA) for Response Surface Model

Source	Sum of squares	*df*	*F* value	*P* value
B	467.87	1	20.66	0.0105
D	423.12	1	17.93	0.0133
AC	342.12	1	14.50	0.0190
B^2	251.30	1	10.65	0.0310
C	83.89	1	3.55	0.1325
A	26.81	1	1.14	0.3465
CD	21.79	1	0.92	0.3911
A^2	17.67	1	0.75	0.4358
D^2	15.39	1	0.65	0.4647
AB	12.46	1	0.54	0.5048
BD	6.73	1	0.28	0.6217
BC	2.63	1	0.11	0.7553
AD	1.60	1	0.068	0.8075
C^2	0.0060	1	2.54E-003	0.9622

df degree of freedom

Decrease of Directional Electric Forces. Collecting fibers between two magnets, instead of usual plate collectors, changes electric field lines direction toward the two magnets as it can be seen in Figure 8. As a result of directional forces applied to charged jet, fibers are tended to align between the magnets.

Equation (5), which is a familiar equation, gives the relation between voltage (V), tip-target distance (d), electric field (E) and the parameter of electric field direction ($\cos\theta$).

$$\Delta V = Ed\cos\theta \tag{5}$$

According to eq. (5), increasing d decreases electric field intensity, in constant voltage. Although farther increase in distance results in smaller $\cos\theta$ ($0 \le \theta \le \pi/2$), the limitation of $\cos\theta$ value range in comparison with d values weakens its role in this equation.

Hence, as it can be seen Figure 5(b), increase in distance gains less alignment especially at high distances.

Solenoid magnetic field could be calculated based on the following equation:

$$B = \mu_0 nI \tag{6}$$

B, n, and I are magnetic field intensity, solenoid coils number and electric current, respectively. More bending instability due to distance increase produces much more coils of jet solenoid. Thus, magnetic field intensity in eq. (3), increases with more n. Yang et al. expressed that interactions between the external applied magnetic field and magnetic field produced by jet movement, is responsible for aligning nanofibers in the gap.[28] Consequently, stronger produced magnetic field, due to jet instability growth, may be effective to gain more alignment. Therefore, that the cause of alignment in increasing part of

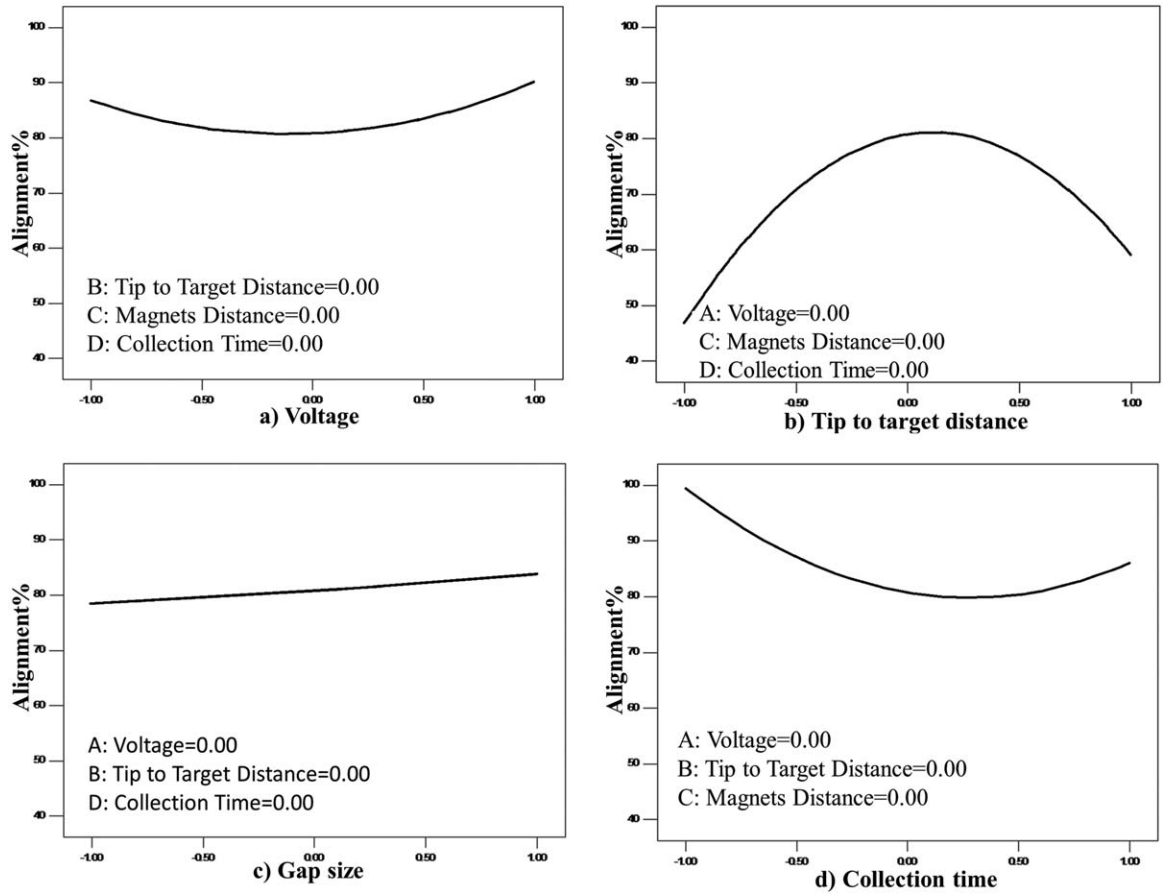

Figure 5. Illustrations of one factor effects, horizontal axes are coded values.

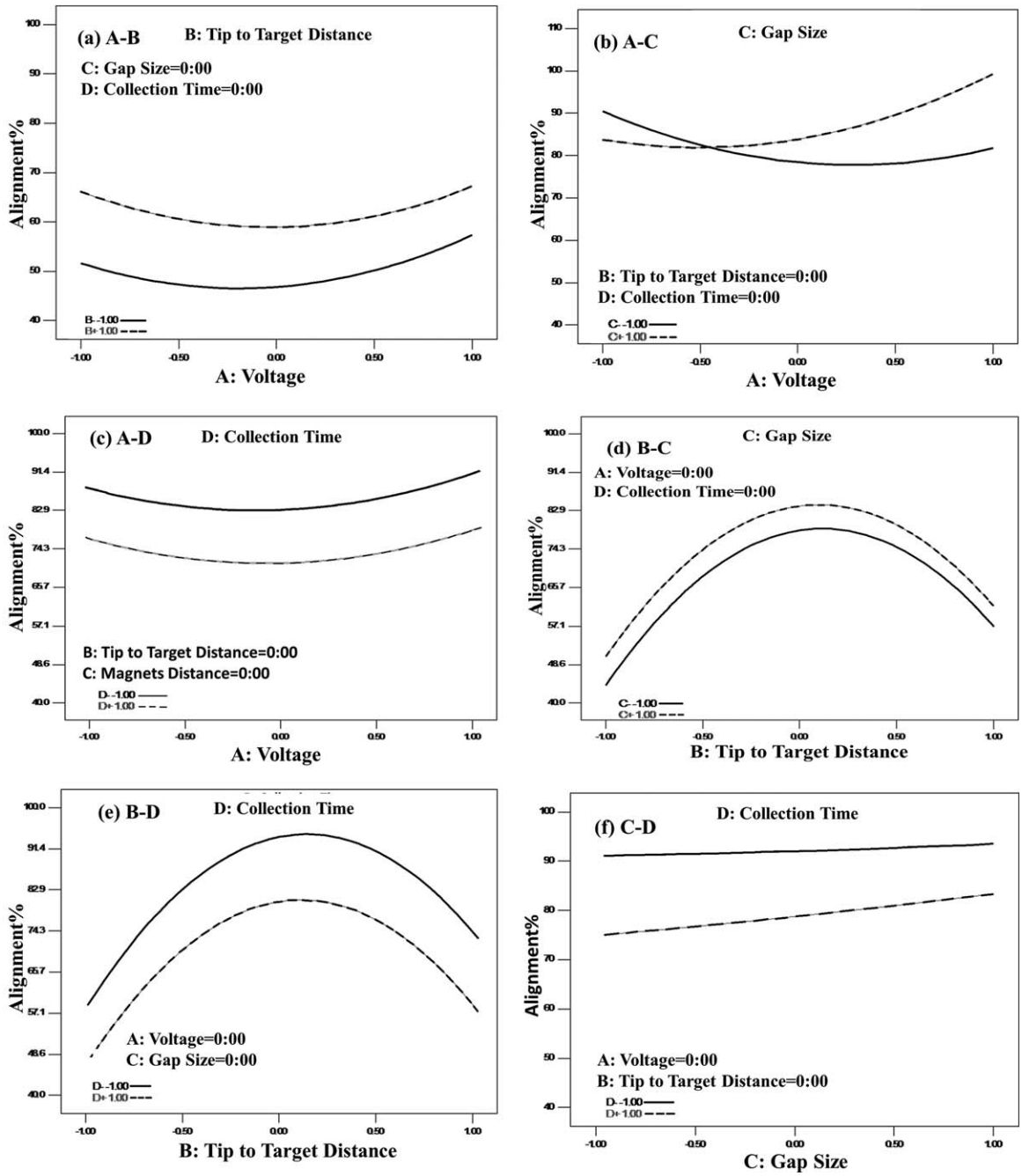

Figure 6. Pairwise interactions of factors, horizontal axes are coded values.

Figure 5(b) with distance is a result of Yang et al. hypothesis although Figure 6(d) does not show any interaction between distance and magnetic field.

Voltage

Nanofibers alignment could be affected by voltage in two ways: electric field and bending instability.

Electric Field. As discussed above, the directional electric field intensity toward the electrodes is cause of aligning nanofibers. This alignment motivation increases in higher voltage values as is indicated in the eq. (5).

Bending Instability. Higher voltage makes more static charges on the jet. Thus, increasing static charges content of the jet leads to increasing jet bending instability which finally decreases nanofibers alignment.

These two mechanisms are in competition with each other. The slightly alternating alignment with voltage in Figure 5(a) is due to this competition. Figure 5(a) illustrates that voltage do not

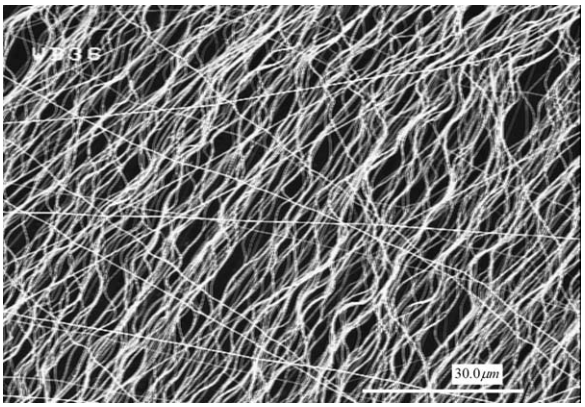

Figure 7. Wavy-shaped nanofibers.

have any considerable increasing or decreasing effects on nanofibers final alignment. This means none of the above way of affections is the conqueror of this competition.

Voltage-gap size interaction (P value = 0.019) is more effective on alignments than voltage (P value = 0.3). Consequently, it can be concluded that voltage effects on alignment through its interaction with magnets gap size. This interaction effect will be explained in next part.

Magnets Gap

Figure 5(c) shows the magnets gap effect on alignment. In less gap sizes, the magnetic field between the two magnets intensifies. This results in more motivation of nanofibers alignment due to stronger magnetic field. On the other hand, at constant distance, decreasing the gap size, increases $\cos\theta$. At constant voltage, according to eq. (5), this lead to less electric field intensity. As discussed above, decreasing electric field has a negative effect on alignment. This description is in conformity Liu et al.[24]

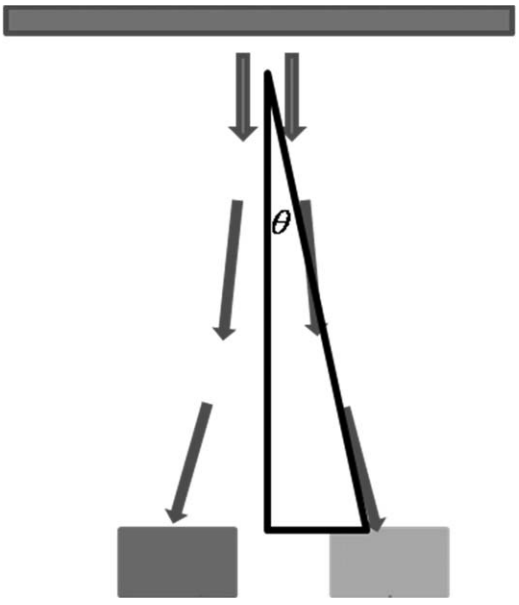

Figure 8. Directional electric field due to using grounded magnets.

Figure 5(a) shows that electric field line distribution changes have slightly more effects on alignment than magnetic field strength changes. It is probable, with using higher values of magnetic field strength magnifies its role in alignment.

Figure 6(b) shows that magnets gap has interaction with voltage and distance. These interactions could be described through the eq. (5). In this equation, $\cos\theta$ changes with gap size. All three factor: voltage, distance and magnetic field line distribution ($\cos\theta$) are in relation with each other in this equation and effect on electric field according to it.

CONCLUSIONS

In this research the mechanisms of external electric and magnetic field effects on nanofibers alignment were discussed. To do so, the three factor of tip to target distance, voltage and magnets distance for investigating effects of above mentioned fields and the factor of collection time were designed to study effects of residual charges on alignment. In this method, 95.3% of PAN nanofibers alignment was obtained. As the statistical results showed, tip to target distance (B: P value = 0.0105) and collection time (D: P value = 0.0133) has considerable effects on alignment. Due to strong interaction between magnetic and electric effects on final alignment, their interaction parameter (AC: P value = 0.0190) has considerable effect on alignment and these two external field effects depends on each other in many aspects and work dependently as discussed.

REFERENCES

1. Fang, J.; Haitao, N.; Tong, L.; Xungai, W. *Chin. Sci. Bull.* **2008**, *53*, 2265.
2. Tan, S.; Huang, X.; Wu, B. *Polym. Int.* **2007**, *56*, 1330.
3. Vasita, R.; Katti, D. S. *Int. J. Nanomed.* **2006**, *1*, 15.
4. Qin, X. H.; Wang, S. Y. *J. Appl. Polym. Sci.* **2006**, *102*, 1285.
5. Luo, Y.; Nartker, S.; Miller, H.; Hochhalter, D.; Wiederoder, M.; Wiederoder, S.; Setterington, E.; Drzal, L. T.; Alocilja, E. C. *J. Appl. Polym. Sci.* **2010**, *26*, 1612.
6. Gorji, M.; Jeddi, A.; Gharehaghaji, A. *J. Appl. Polym. Sci.* **2012**, *125*, 4135.
7. Thavasi, V.; Singh, G.; Ramakrishna, S. *Energy Environ. Sci.* **2008**, *1*, 205.
8. Phillip, P.; Gibson, H. S.; Rivin, D. *Colloid. Surf. A* **2001**, *187*, 469.
9. Ramakrishna, S.; Fujihara, K.; Teo, W.; Lim, T; Ma, Z. An Introduction to Electrospinning and Nanofibers; World Scientific Publishing Co. Pte.: Singapore, **2005**.
10. Reneker, D. H.; Yarin, A. L.; Fong, H.; Koombhongse, S. *J. Appl. Phys.* **2000**, *87*, 4531.
11. Hohman, M.; Shin, Y.; Rutledge, G.; Brenner, M. *J. Phys. Fluids* **2001**, *13*, 2201.
12. Yang, D.; Zhang, J.; Zhang, J.; Nie, J. *J. Appl. Polym. Sci.* **2008**, *110*, 3368.
13. Ren, Z. F.; Liu, B. Z.; Liu, G. Q.; Kanga, Y.; Fana, H.; Li, H. *J. Text. Inst.* **2010**, *101*, 571.

14. Reneker, D. H.; Yarin, A. L.; Fong, H.; Koombhongse, S. *J. Appl. Phys.* **2000**, *87*, 4531.
15. Teo, W. E.; Ramakrishna, S. *Nanotechnology* **2006**, *17*, 89.
16. Zhou, Z. P.; Lai, C. L.; Zheng, L. F.; Qiam, Y.; Hou, H. Q.; Fong, H.; Reneker, D. H. *Polymer* **2009**, *50*, 2999.
17. Zhou, Z. P.; Liu, K. M.; Lai, C. L.; Li, J. H.; Hou, H. Q.; Reneker, D. H.; Fong, H. *Polymer* **2010**, *51*, 2360.
18. Kowalewski, T. A.; Blonski, S.; Barral, S. *Bull. Pol. Acad. Sci. Tech.* **2005**, *53*, 385.
19. Zussman, E.; Rittel, D.; Yarin, A. L. *Appl. Phys. Lett.* **2003**, *82*, 3958.
20. Xu, C. Y.; Inai, R.; Kotaki, M.; Ramakrishna, S. *Biomaterials* **2004**, *25*, 877.
21. Zussman, E.; Theron, A.; Yarin, A. L. *Appl. Phys. Lett.* **2003**, *82*, 973.
22. Katta, P.; Alessandro, M.; Ramsier, R. D.; Chase G. *Nano Lett.* **2004**, *4*, 2215.
23. Li, D.; Wang, Y.; Xia, Y. *Nano Lett.* **2008**, *3*, 1167.
24. Liu, L.; Dzenis, Y. A. *Nanotechnology* **2008**, *19*, 355307.
25. Dalton, P. D.; Klee, D.; Moller, M. *Polymer* **2005**, *46*, 611.
26. Chuanqchote, S.; Supaphol, P. *J. Nanosci. Nanotechnol.* **2006**, *6*, 125.
27. Yang, D.; Lu, B.; Zhao, Y.; Jiang, X. *Adv. Mater.* **2007**, *19*, 3702.
28. Yang, D.; Zhang, J.; Zhang. J.; Nie, J. *J. Appl. Polym. Sci.* **2008**, *110*, 3368.
29. Li, P.; Liu, C.; Song, Y.; Niu, X.; Liu, H.; Fan, Y. *J. Nanomater.* **2013**, 2013, 1.
30. Linyu, M.; Rui, H.; Yanfang, G.; Yizheng. F.; Yaqing, L. *J. Wuhan Univ. Technol. Mater. Sci. Ed.* **2013**, *28*, 1107.
31. Badrossamay, M. R.; Mcllwee, H. A.; Goss. J. A.; Parker, K. K. *Nano Lett.* **2010**, *10*, 2257.
32. Grasl, C.; Arras, M. M. L.; Stoiber, M.; Bergmeister, H.; Schima, H. *Appl. Phys. Lett.* **2013**, *102*, 053111.
33. Liu, Y.; Zhang, X.; Xia. Y.; Yang, H. *Adv. Mater.* **2010**, *22*, 2454.
34. Coles, S. R.; Jacobs, D. R.; Meredith, J. O.; Barker, G.; Clark, A. J.; Kirwan, K.; Stanger, J.; Tucker, N. *J. Appl. Polym. Sci.* **2010**, *117*, 2251.
35. Cui, W.; Li, X.; Zhou, S.; Weng, J. *J. Appl. Polym. Sci.* **2007**, *103*, 3105.
36. Ledolter, J. *Qual. Technol. Quant. Manag.* **2011**, *8*, 183.
37. Kim, K. W.; Lee, K. H.; Khil, M. S.; Ho, Y. S.; Kim, H. Y. *Fibers Polym.* **2004**, *5*, 122.
38. Bazbouz, M. B.; Stylios, G. K.; *J. Appl. Polym. Sci.* **2008**, *107*, 3023.
39. Yang, D.; Lu, B.; Zhao, Y.; Jiang, X.; *Adv. Mater.* **2007**, *19*, 3702.
40. Yan, H.; Liu, L.; Zhang, Z. *Appl. Phys. Lett.* **2009**, *95*, 14314.
41. Jalili, R.; Morshed, M.; Ravandi, S. *J. Appl. Polym. Sci.* **2006**, *101*, 4350.
42. Acharya, M.; Arumugam, G. K.; Heiden, P. A. *Macromol. Matter. Eng.* **2008**, *293*, 666.
43. Pokorny, M.; Niedoba, K.; Velebny, V. *Appl. Phys. Lett.* **2010**, *96*, 193111.
44. Fallahi, D.; Rafizadeh, M.; Mohammadi, N.; Vahidi, B. *J. Polym. Eng. Sci.* **2010**, *50*, 1372.